

## SUPPLEMENTAL MATERIAL

for Müller et al.

### *Mass determination by light scattering analysis*

Ribosomes, ribosomal subunits, and Sec62N were characterized by asymmetric-flow field-flow fractionation (Eclipse 2, Wyatt Technology) and online multi-angle light scattering analysis (miniDAWN Tristar and QELS, Wyatt Technology), 280 nm UV absorbance (Agilent 1100 series), and refractive index-measurements (Shodex RI-101). Samples were applied by autosampler (Agilent 1100 series). Ribosomes were fractionated in 20 mM HEPES-KOH, pH 7.6, 50 mM KCl, 2 mM MgCl<sub>2</sub>. Ribosomal subunits were fractionated in 20 mM HEPES-KOH, pH 7.6, 1 M KCl, 2 mM MgCl<sub>2</sub>, 1 mM DTT. Sec62N was fractionated in 50 mM Tris-HCl, pH 8, 300 mM NaCl. The data were analyzed with ASTRA software version 5.3.2.16 (Wyatt Technology) and a value for  $dn/dc$  for protein of 0.185 ml/g. Molecular mass and hydrodynamic radius of the purified 80S ribosomes were determined as  $3.62 \pm 0.15$  MDa and  $18.25 \text{ nm} \pm 1.71$ , of 60S as subunits  $2.5 \pm 0.03$  MDa and  $14.45 \pm 0.36$  nm, and of 40S subunits as  $1.4 \pm 0.01$  MDa and  $7.54 \pm 0.43$  nm; molecular mass of purified Sec62N was determined as 35 kDa (Supplemental Figures 1 and 2).

### *Interaction of human Sec62 and Sec63 involves the carboxyterminus of Sec63 and the central region of Sec62N*

Peptide spots that corresponded to Sec62 and Sec63C, respectively, were synthesized on cellulose membranes according to established procedure (Frank, 1992). Subsequently, the membranes were incubated with <sup>14</sup>C-labeled Sec63C, Sec63C26, or Sec62N under the conditions of the pull down assay. The bound proteins were visualized by phosphorimaging and plotted against the respective protein sequence (Supplemental Figures 3 and 4). Upon incubation of the Sec62 membrane with Sec63C or Sec63C26, a highly polar and overall

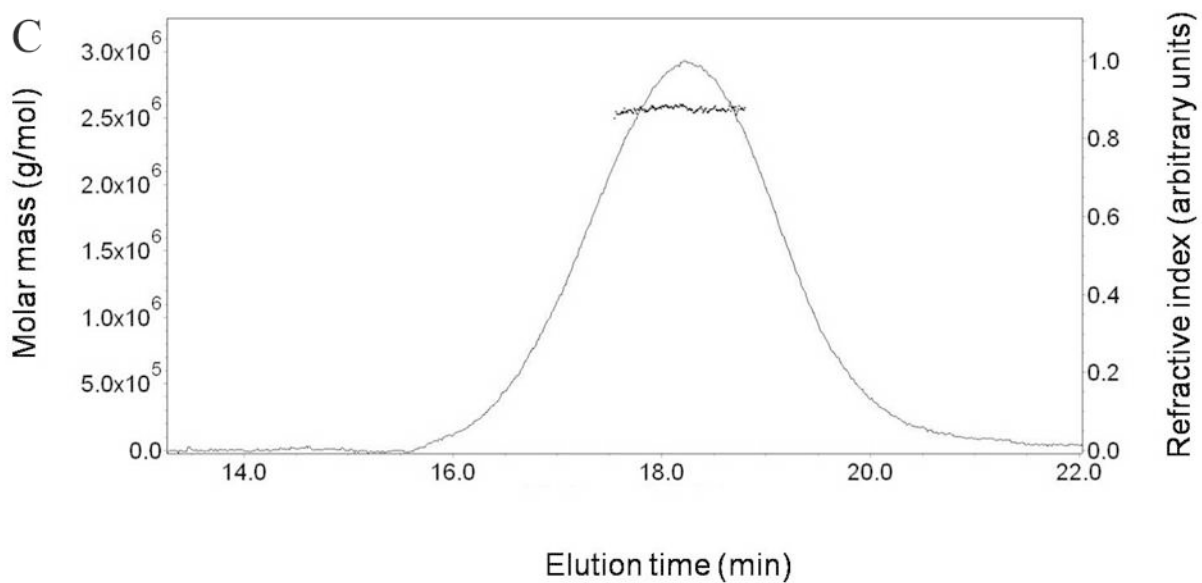
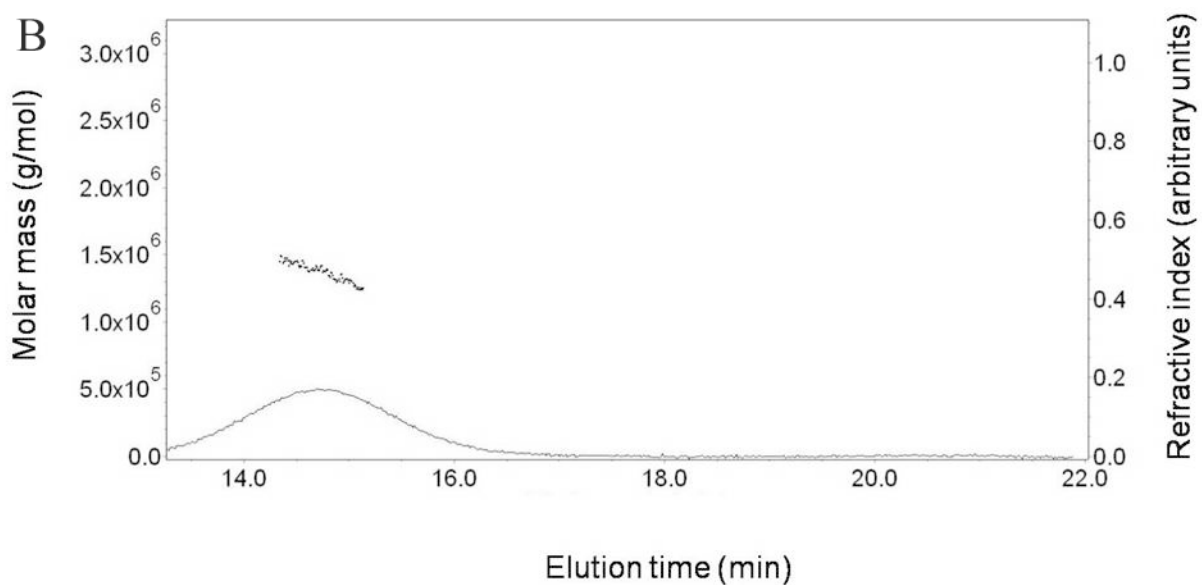
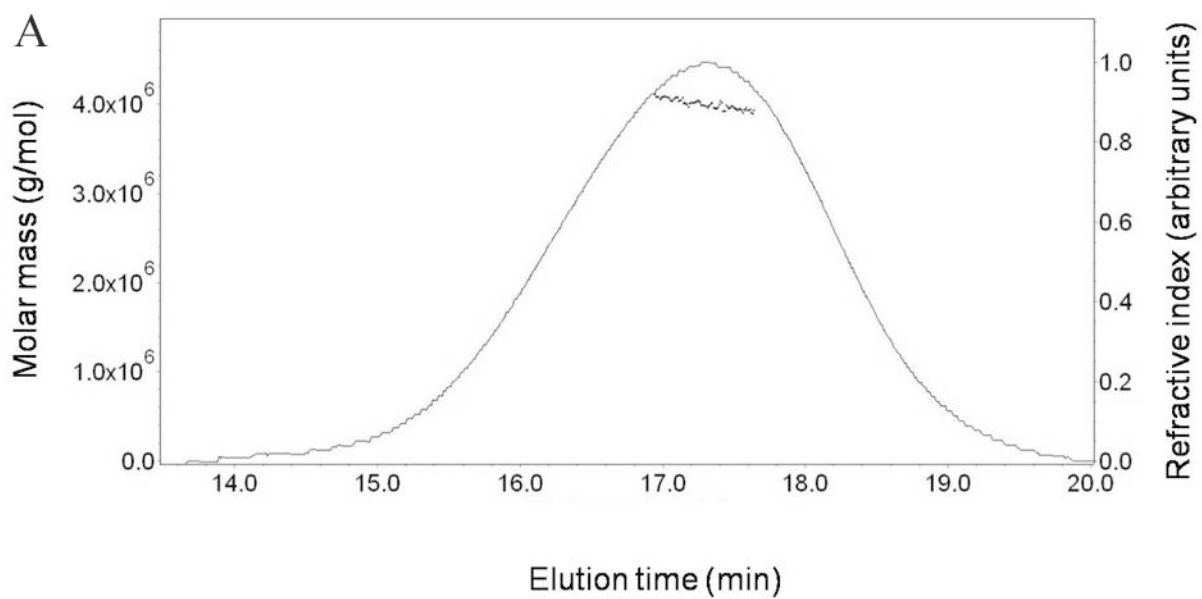
positively charged section within Sec62N was identified as dominant interaction site (amino acid residues 96-145). We note that the aminoterminal oligopeptide, involved in ribosome binding of Sec62N, did not significantly interact with Sec63C or Sec63C26. When the Sec63C membrane was probed with Sec62N, the carboxyterminal region of Sec63C was identified as the predominant binding site. Thus these results confirmed the pull down and peptide competition experiments that are shown in Figure 2.

### ***Mammalian Sec62 inhibits translation in the presence of microsomes***

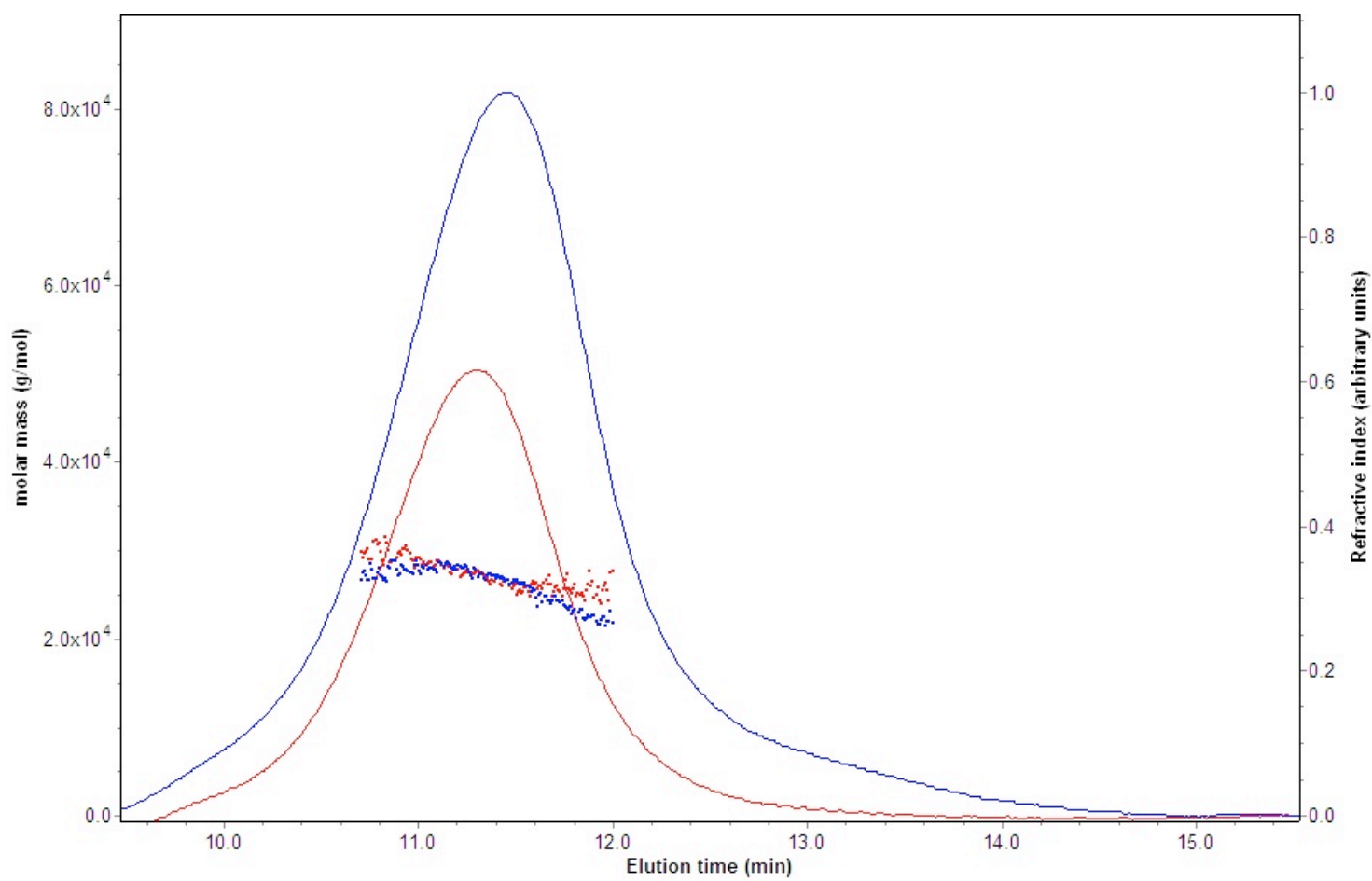
Sec62N was also tested for its ability to inhibit synthesis of firefly luciferase or bovine preprolactin in the presence of canine pancreatic microsomes (Supplemental Figure 5, A and B). In this assay, Sec62N was active in inhibiting protein synthesis, too. We note that preprolactin was not affected by Sec62N with respect to its transport into microsomes.

### ***Sequence comparison***

The sequences of canine Sec62, Sec63, and ERj1, respectively, were used for BLAST database searches. The identified orthologs in *Homo sapiens*, *Mus musculus*, *Gallus gallus*, *Xenopus laevis*, *Caenorhabditis elegans*, *Drosophila melanogaster*, *Trypanosoma brucei*, *Saccharomyces cerevisiae*, *Arabidopsis thaliana*, and *Oryza sativa* are shown in Supplemental Figures 6 through 8.

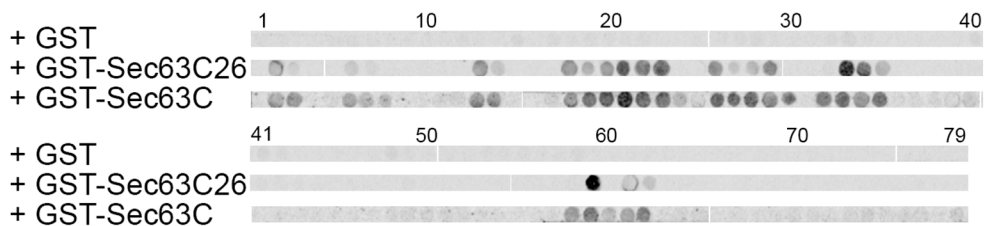


Supplemental Figure 1. Molecular mass of canine ribosomes and their subunits. Ribosomes were purified from canine pancreas and washed with high salt and puromycin. Ribosomal subunits were prepared by sucrose gradient centrifugation. Ribosomes (270  $\mu\text{g}$ , A), 40S-subunits (36  $\mu\text{g}$ , B), and 60S-subunits (169  $\mu\text{g}$ , C) were fractionated in 20 mM HEPES-KOH, pH 7.6, 50 mM KCl, 2 mM  $\text{MgCl}_2$  (80S) and 20 mM HEPES-KOH, pH 7.6, 1 M KCl, 2 mM  $\text{MgCl}_2$ , 5 mM DTT (60S, 40S), respectively, on a cellulose membrane (cut off: 5 kDa, spacer 350  $\mu\text{m}$ ) with a channel flow of 1 ml/min and a cross flow of 1 ml/min. The continuous trace refers to the refractive index. In the peak area, molar mass was calculated for each individual data set from the multi-angle light scattering monitor. We note that a horizontal line for the molar mass values indicates that a homogeneous/monodispers sample was analyzed.

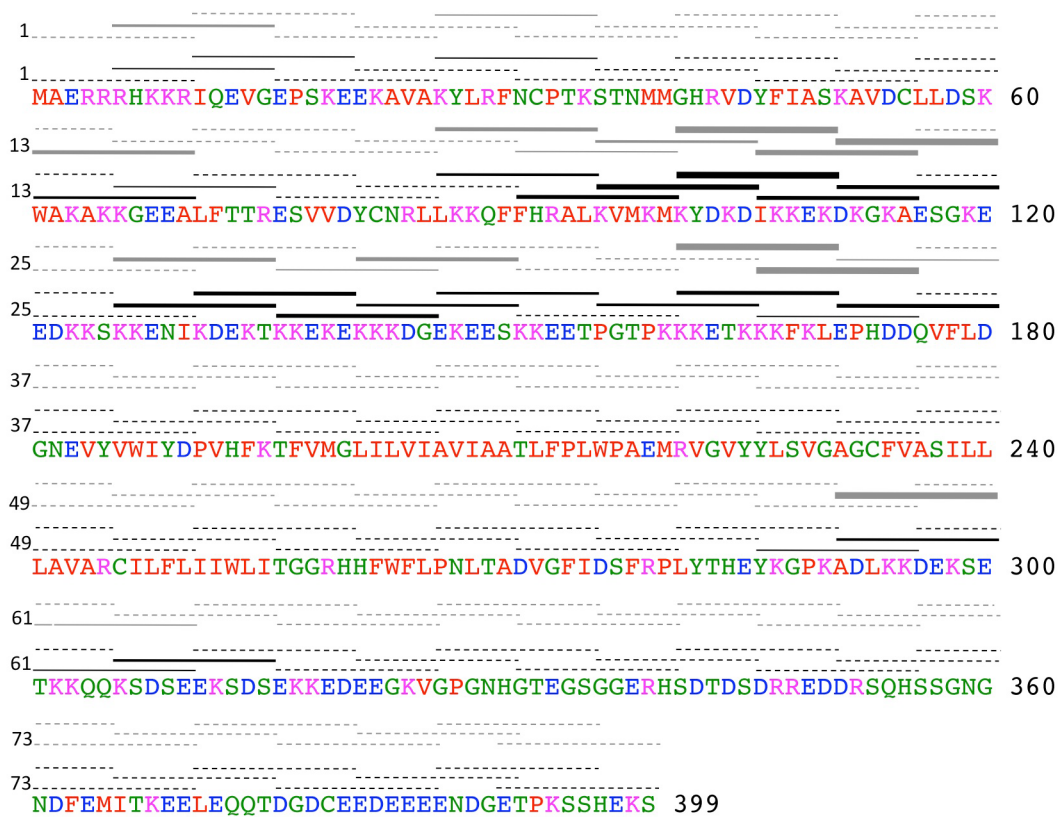


Supplemental Figure 2. Molecular mass of purified human Sec62N. Sec62N was purified from *E. coli* cells. Sec62N (10 and 20  $\mu\text{g}$ , respectively) was fractionated in 50 mM Tris-HCl, pH 8, 300 mM NaCl on a cellulose membrane (cut off: 5 kDa, spacer 350  $\mu\text{m}$ ) with a channel flow of 1 ml/min and a cross flow of 3 ml/min. The two analyses were compiled in a single graph and are differentiated by colours (10  $\mu\text{g}$ , red; 20  $\mu\text{g}$ , blue). The continuous traces refer to the refractive index. In the peak areas, molar masses were calculated for each individual data set from the multi-angle light scattering monitor. We note that a horizontal line for the molar mass values indicates that a homogeneous/monodispers sample was analyzed.

A)

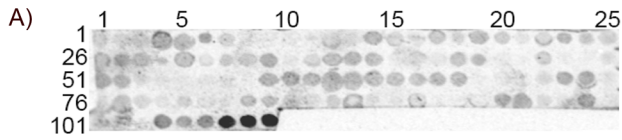


B)



Supplemental Figure 3. Interaction of human Sec62 and Sec63 involves the central region of Sec62N. Peptide spots (10-mers, overlapping by 5 amino acid residues) that corresponded to Sec62 were synthesized on cellulose membranes according to established procedure (Frank, 1992). Subsequently, the membranes were incubated with <sup>14</sup>C-labeled GST, GST-Sec63C, or GST-Sec63C26. The bound proteins were visualized by phosphorimaging (A) and plotted against the Sec62 sequence (B). The lines refer to spots (grey, GST-Sec63C26; black, GST-Sec63C). The line thickness refers to signal intensity, the colours of amino acid residues refer to polarity. Small numbers indicate the respective peptide spot, large numbers indicate the amino acid residue in the sequence (B).





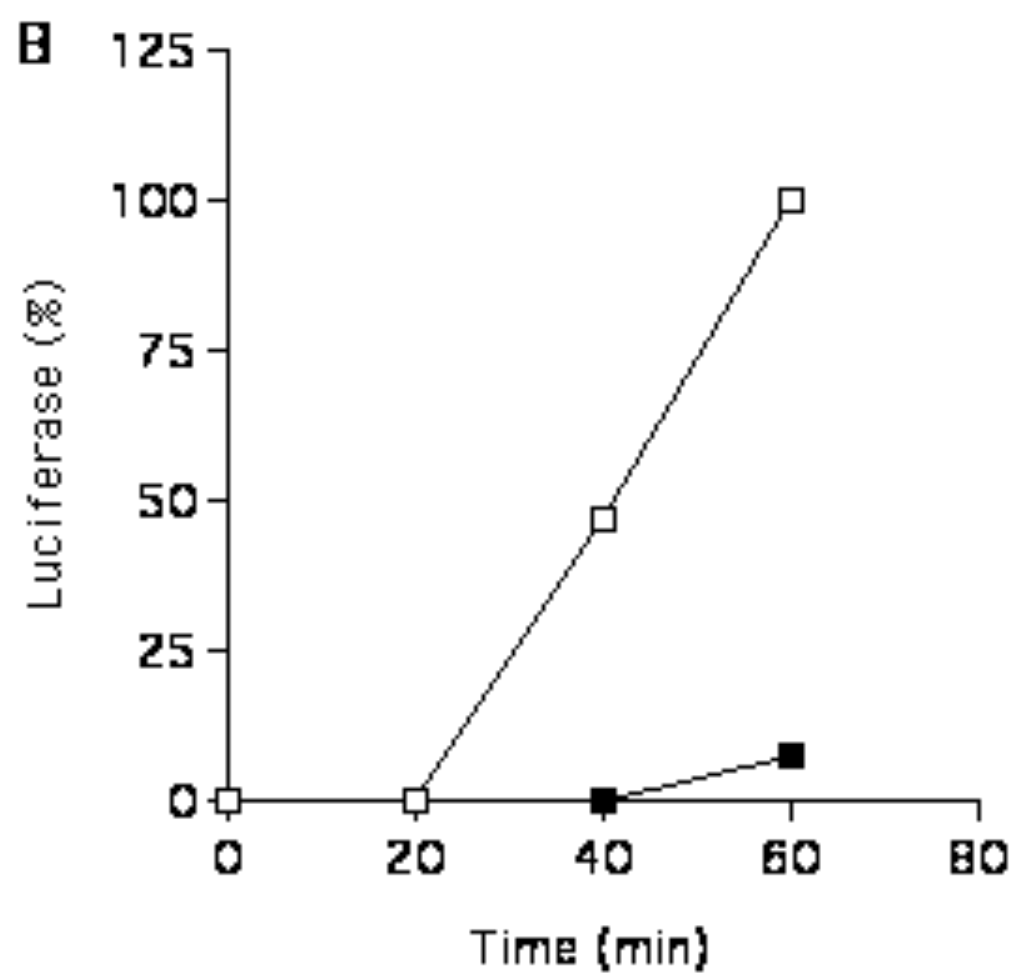
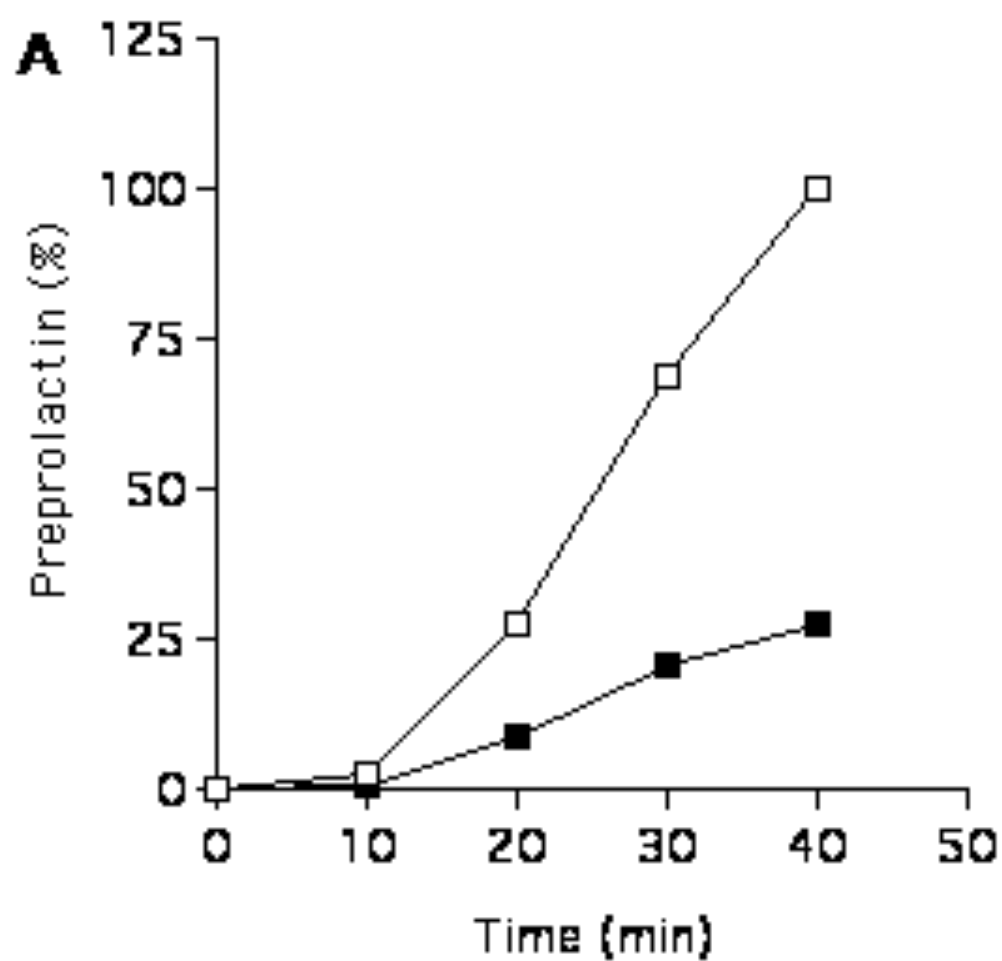
B)

```

1 1 SWWYRSIRYSGDQILIRTTQIYTYFVYKTRNMDMKRLIMVLAGASEFDPQYNKDATS RPT 269
6 11
16 21
DNILIPQLIREIGSINLKKNEPPLTCPYSLKARVLLLSHLARMKIPETLEEDQQFMLKKC 329
26 31 36
PALLQEMVNVICQLIVMARNREEREFRAPTLASLENCMKLSQMAVQGLQQFKSPLLQLPH 389
41 46
IEEDNLRRVSNHKKYKIKTIQDLVSLKESDRHTLLHFLEDEKYEEVMAVLGSFPYVTMDI 449
51 56
KSQVLDEEDSNNITVGS�VTVLVKLTROTMAEVFEKEQSICAAEEQPAEDGQGETNKNRT 509
61 66 71
KGGWQQKSKGPKKTAKSKKKKPLKKKPTPVLLPQSKQQKQKQANGVVGNEAAVKEDDEEV 569
76 81
SDKGS DSEEEETNRDSQSEKDDGSDRDSREQDEKQNKDDEAEWQELQQS IQRKERALLE 629
86 91 96
TKSKITHPVYSLYFPEEKQEWWWLYIADRKEQTLISMPYHVCTLKDTEEVELKFPAPGKP 689
101 106
GNYQYTVFLRSDSYMGLDQIKPLKLEVHEAKPVPENHPQWDTAIEGDEDQEDSEGFEDSF 749
EEEEEEEEDD 760

```

Supplemental Figure 4. Interaction of human Sec62 and Sec63 involves the carboxyterminus of Sec63. Peptide spots (15-mers, overlapping by 10 amino acid residues) that corresponded to Sec63C were synthesized on cellulose membranes according to established procedure (Frank, 1992). Subsequently, the membranes were incubated with <sup>14</sup>C-labeled Sec62N. The bound proteins were visualized by phosphorimaging (A) and plotted against the Sec63C sequence (B). The lines refer to spots, the colours of amino acid residues refer to polarity. The line thickness refers to signal intensity. Small numbers indicate the respective peptide spot, large numbers indicate the amino acid residue in the sequence (B).



Supplemental Figure 5. Mammalian Sec62 inhibits translation in the presence of microsomes. Preprolactin (A) or luciferase (B) were synthesized in reticulocyte lysate in the presence of [<sup>35</sup>S]methionine and canine pancreatic microsomes. The translation reactions were supplemented with buffer (open squares) or recombinant protein (filled squares; 1 μM) in the same buffer. After the indicated incubation times, aliquots of the complete translation reactions were subjected to SDS-PAGE and phosphorimaging. The amount of preprolactin or luciferase that was present at the end of the buffer control reaction was set to 100 percent.



Supplemental Figure 6. Sequence alignment for Sec62 proteins. The alignment was created with the MegAlign option of the DNASTAR sequence analysis software, version 7.1.1 (Clustal V, PAM 250). The most conserved regions were boxed. The basic oligopeptides (green shading) and the predicted transmembrane domains (yellow shading) are indicated. The sequences were taken from the following accession numbers: *Homo sapiens* (AAB51391), *Canis lupus familiaris* (XP\_851757), *Mus musculus* (AAH67202), *Gallus gallus* (NP\_001012620), *Xenopus laevis* (NP\_001086825), *Caenorhabditis elegans* (NP\_495908), *Drosophila melanogaster* isoform B (AAO39524), *Saccharomyces cerevisiae* (CAB56541), *Arabidopsis thaliana* (NP\_001030734), and *Oryza sativa* (EEE56884). We note that there is no Sec62 ortholog in *Trypanosoma brucei* (also see reference 10). Furthermore, we note that there also is a isoform A in *Drosophila melanogaster* that differs from isoform B (AAO39524) in the amino terminal peptide (MSEKKRARRRKD instead of MSGEEEYFGE EEEEEGEGDIYDDGT).







	810	820	830	840	850	860	870	
hsSec63	MFLRSDSYMGLDQIKPLKLEVHERKPVF	ENHPQNDTRIEGDEDDQEDS	EGFEDSFEEEEEEEDDD					760
cfSec63	MFLRSDSYMGLDQIKPLKLEVHERKPVF	ENHPQNDTRIEGDEDDQEDS	EGFEDSFEEEEEEEDDD					760
mmSec63	MFLRSDSYMGLDQIKPLKLEVHERKPVF	ENHPQNDTRIEGDEDDQEDS	EGFEDSFEEEEEEEDDD					760
ggSec63	MFLRSDSYMGLDQIKPLKLEVHERKPVF	ENHPQNDTRIEGDEDDQEDS	EGFEDSFEEEEEEEDDD					759
xlSec63	MFLRSDSYMGLDQIKPLKLEVHERKPVF	ENHPQNDTRIEGDEDDQEDS	EGFEDSFEEEEEEEDDD					755
ceSec63	LSWKSDSYMDREYSVDFKIDAKRAKFM	IKDDYVDEIDRVEV	SSDDYVTGDDSD					752
dnSec63	MCRLRSQSYLIDGQDCELKIDVOKRFP	TDLPQDISESEPHTDQQ	ENLSDYTTDTSD					753
tbSec63	KIMK-NML	QIMQVSKNE	ALLKASLRAL					490
scSec63	QIVKIDTDFTTDLDITMINKVRSDFAEQV	EVYSEEDDEVSTDDDETE	SDASDYTDIDDTD					663
atSec63	GENAEE	QVEE	DDDEIE	EDVESEVSE	EDDKKRGSKKKV	NKSSSE	ESGSDEE	661
osSec63	GPVARE	QVEE	EEEEEE	EDVDESEVSD	EDDKKRGKGVAN	VAHQKANS	IDSGSD	681

Supplemental Figure 7. Sequence alignment for Sec63 proteins. The alignment was created with the MegAlign option of the DNASTAR sequence analysis software, version 7.1.1 (Clustal V, PAM 250). The most conserved regions were boxed. The J-domain (blue shading) and the predicted transmembrane domains (yellow shading) are indicated. The sequences were taken from the following accession numbers: *Homo sapiens* (AAC83375), *Canis lupus familiaris* (XM\_532252), *Mus musculus* (AAK00580), *Gallus gallus* (XP\_419802), *Xenopus laevis* (AAI10928), *Caenorhabditis elegans* (NM\_061062), *Drosophila melanogaster* (AAF50571), *Trypanosoma brucei* (XM\_822206), *Saccharomyces cerevisiae* (CAA99476), *Arabidopsis thaliana* (NP\_001117623), and *Oryza sativa* (NM\_001058956).



	490	500	510	520	530	540	550	560	
HsERj1	---RTRKQPEPEEKSRKPKRQKDFDISEQNES---	SDDESLRKEFASRAE	EWNTQNOOKLLELALQOMPESSEDRWIKIAR						526
CfERj1	---RAAKVEPEEKFRGKPKQKDFDISEQNES---	SDDESQKKDPTAAAE	EWNTQNOOKLLELALQOMPKGSEDRWIKIARK						533
MmERj1	---RMTKVEPEEKLRGKPKQKDFDISEQNDG---	SDDEKQKERTAAAE	EWNTQNOOKLLELALQOMPKGSEDRWIKIARK						524
GgERj1	MMFRAATKVEVSEKGRGPKQKDFDNTEDQEE---	SDDESRKFEKRALE	ELATQNOOKLLELALQOMPKGTSDRWIKIARK						478
XlERj1	ERASSSRGVEEKVGRGPKQKDFDTEQEAELGDSNDMRAKEDSS---	SDLSQNOOKLLELALQOMPKGTEGDRWIKIARK							506
CeERj1	-----EEK-----	SDDSQREKAFETALQOMPKGTEGDRWIKIARK							386
DmERj1	SVPEKTKVEELVRYRYKYLCELVKTKKRAEENEPEDAAAIIEELPEEELAPPEPEVAPAEKKLSTREDRRKA---								505

	570	580	
HsERj1	WPSKSKEDCIRYKLLVELVOKKKQAKS		554
CfERj1	WPSKSKEDCIRYKLLVELVOKKKQAKS		561
MmERj1	WPSKSKEDCIRYKLLVELVOKKKQAKS		552
GgERj1	WPKSKKEICIRYVLLVELVOKKKQAKS		506
XlERj1	WPKSKEDCIRYKLLVELVOKKKQAKS		534
CeERj1	IGKTKKQMMERKQARIMIRKKTNDT		414
DmERj1	DLSSQESDRAIQVEI		522

Supplemental Figure 8. Sequence alignment for ERj1/DnaJC1 proteins. The alignment was created with the MegAlign option of the DNASTAR sequence analysis software, version 7.1.1 (Clustal V, PAM 250). The most conserved regions were boxed. The signal peptide (red shading), the J-domain (blue shading), the predicted transmembrane domain (yellow shading), the basic oligopeptide (green shading), and the predicted Myb-domains (orange shading) are indicated. The sequences were taken from the following accession numbers: *Homo sapiens* (NP\_071760), *Canis lupus familiaris* (XM\_844389), *Mus musculus* (NP\_031895), *Gallus gallus* (XM\_418609), *Xenopus laevis* (AAH73404), *Caenorhabditis elegans* (NM\_066548), *Drosophila melanogaster* (NM\_133126). We failed to identify any orthologs of ERj1 in *Trypanosoma brucei*, *Saccharomyces cerevisiae*, *Arabidopsis thaliana*, and *Oryza sativa*.